UPSCALING MULTIPHASE FLOW IN POROUS MEDIA

Upscaling Multiphase Flow in Porous Media

From Pore to Core and Beyond

Edited by

D.B. DAS
University of Oxford, U.K.

and

S.M. HASSANIZADEH
Utrecht University, The Netherlands

Part of this volume has been published in the Journal Transport in Porous Media vol. 58, No. 1–2 (2005)

Springer

A C.I.P. Catalogue record for this book is available from the Library of Congress.

ISBN 1-4020-3513-6 (HB)

Published by Springer,
P.O. Box 17, 3300 AA Dordrecht, The Netherlands.

Sold and distributed in North, Central and South America
by Springer,
101 Philip Drive, Norwell MA 02061, U.S.A.

In all other countries, sold and distributed
by Springer,
P.O. Box 322, 3300 AH Dordrecht, The Netherlands.

Printed on acid-free paper

Printed in the Netherlands

To our mothers:
Renuka and Tajolmolouk

And our fathers:
Kula and Asghar

Table of Contents

Editorial

Multiphase flow in porous media is an extremely important process in a number of industrial and environmental applications, at various spatial and temporal scales. Thus, it is necessary to identify and understand multiphase flow and reactive transport processes at microscopic scale and to describe their manifestation at the macroscopic level (core or field scale). Current description of macroscopic multiphase flow behavior is based on an empirical extension of Darcy's law supplemented with capillary pressure-saturation-relative permeability relationships. However, these empirical models are not always sufficient to account fully for the physics of the flow, especially at scales larger than laboratory and in heterogeneous porous media. An improved description of physical processes and mathematical modeling of multiphase flow in porous media at various scales was the scope a workshop held at the Delft University of Technology, Delft, The Netherlands, 23–25 June, 2003. The workshop was sponsored by the European Science Foundation (ESF). This book contains a selection of papers presented at the workshop. They were all subject to a full peer-review process. A subset of these papers has been published in a special issue of the journal *Transport in Porous Media* (2005, Vol. 58, nos. 1–2).

The focus of this book is on the study of multiphase flow processes as they are manifested at various scales and on how the physical description at one scale can be used to obtain a physical description at a higher scale. Thus, some papers start at the pore scale and, mostly through pore-scale network modeling, obtain an average description of multiphase flow at the (laboratory or) core scale. It is found that, as a result of this upscaling, local-equilibrium processes may require a non-equilibrium description at higher scales. Some other papers start at the core scale where the medium is highly heterogeneous. Then, by means of upscaling techniques, an equivalent homogeneous description of the medium is obtained. A short description of the papers is given below.

Dahle, Celia, and Hassanizadeh present the simplest form of a pore-scale model, namely a bundle of tubes model. Despite their extremely simple nature, these models are able to mimic the major features of a porous medium. In fact, due to their simple construction, it is possible to reveal subscale mechanisms that are often obscured in more complex models. They use their model to demonstrate the pore-scale process that underlies dynamic capillary pressure effects.

Valvatne, Piri, Lopez and Blunt employ static pore-scale network models to obtain hydraulic properties relevant to single, two- and three-phase flow for a variety of rocks. The pore space is represented by a topologically disordered lattice of pores connected by throats that have angular cross sections. They consider single-phase flow of non-Newtonian as well as Newtonian fluids. They show that it is possible to use easily acquired data to estimate difficult-to-measure properties and to predict trends in data for different rock types or displacement sequences.

The choice of the geometry of the pore space in a pore-scale network model is very critical to the outcome of the model. In the paper by *Kainourgiakis, Kikkinides, Galani, Charlambopolous, and Stubos,* a procedure is developed for the reconstruction of the porous structure and the study of transport properties of the porous medium. The disordered structure of porous media, such as random sphere packing, Vycor glass, and North Sea chalk, is represented by three-dimensional binary images. Transport properties such as Kadusen diffusivity, molecular diffusivity, and permeability are determined through virtual (computational) experiments.

The pore-scale network model of Kainourgiakis *et al*. is employed by *Yiotis, Stubos, Boudouvis, Tsimpanogiannis, and Yortsos* to study drying processes in porous media. These include mass transfer by advection and diffusion in the gas phase, viscous flow in the liquid and gas phases, and capillary effects. Effects of films on the drying rates and phase distribution patterns are studied and it is shown that film flow is a major transport mechanism in the drying of porous materials.

Panfilov and Panfilova also start with a pore-scale description of two-phase flow, based on Washburn equation for flow in a tube. Subsequently, through a conceptual upscaling of the pore-scale equation, they develop a new continuum description of two-phase. In this formulation, in addition to the two fluid phases, a third continuum, representing the meniscus and called the M-continuum, is introduced. The properties of the M-continuum and its governing equations are obtained from the pore-scale description. The new model is analyzed for the case of one-dimensional flow. The remaining papers in this book regard upscaling from core scale and higher.

A procedure for upscaling dynamic two-phase flow in porous media is discussed by *Manthey, Hassanizadeh, and Helmig*. Starting with the Darcian description of two-phase flow in a (heterogeneous) porous medium, they perform fine-scale simulations and obtain macro-scale effective properties through averaging of numerical results. They focus on the study of an extended capillary pressure-saturation relationship that accounts for dynamic effects. They determine the value of the dynamic capillary pressure coefficient at various scales. They investigate the influence of averaging domain size, boundary conditions, and soil parameters on the dynamic coefficient.

The dynamic capillary pressure effect is also the focus of the paper by *Nieber, Dautov, Egorov, and Sheshukov*. They analyze a few alternative formulations of unsaturated flow that account for dynamic capillary pressure. Each of the alternative models is analyzed for flow characteristics under gravity-dominated conditions by using a traveling wave transformation for the model equations. It is shown that finger flow that has been observed during infiltration of water into a (partially) dry zone cannot be modeled by the classical Richard's equation. The introduction of dynamic effects, however, may result in unstable finger flow under certain conditions.

Nonequilibrium (dynamic) effects are also investigated in the paper by *Tavassoli, Zimmerman, and, Blunt*. They study counter-current imbibition, where the flow of a strongly wetting phase causes spontaneous flow of the nonwetting phase in the opposite direction. They employ an approximate analytical approach to derive an expression for a saturation profile for the case of non-negligible viscosity of the nonwetting phase. Their approach is particularly applicable to waterflooding of hydrocarbon reservoirs, or the displacement of NAPL by water.

In the paper by *Pickup, Stephen, Ma, Zhang and Clark,* a multistage upscaling approach is pursued. They recognize the fact that reservoirs are composed of a variety of rock types with heterogeneities at a number of distinct length scales. Thus, in order to upscale the effects of these heterogeneities, one may require a series of stages of upscaling, to go from small-scales (mm or cm) to field scale. They focus on the effects of steady-state upscaling for viscosity-dominated (water) flooding operations.

Gielen, Hassanizadeh, Leijnse, and Nordhaug present a dynamic pore-scale network model of two-phase flow, consisting of a three-dimensional network of tubes (pore throats) and spheres (pore bodies). The flow of two immiscible phases and displacement of fluid–fluid interface in the network is determined as a function of time using the Poiseuille flow equation. They employ their model to study dynamic effects in capillary pressure-saturation relationships and determine the value of the dynamic capillary pressure coefficient. As expected, they find a value that is one to two orders of magnitude larger than the value determined by Dahle *et al.* for a much simpler network model.

Eichel, Helmig, Neuweiler, and Cirpka present an upscaling method for two-phase in a heterogeneous porous medium. The approach is based on a percolation model and volume averaging method. Classical equations of two-phase flow are assumed to hold at the small (grid) scale. As a result of upscaling, the medium is replaced by an equivalent homogeneous porous medium. Effective properties are obtained through averaging results of fine-scale numerical simulations of the heterogeneous porous medium. They apply their upscaling technique to experimental data of a DNAPL infiltration experiment in a sand box with artificial sand lenses.

The editors wish to acknowledge an Exploratory Workshop Grant awarded by the European Science Foundation under its annual call for workshop funding in Engineering and Physical Sciences, which made it possible to organize the Workshop on Recent Advances in Multiphase Flow and Transport in Porous Media. We would like to express our sincere gratitude to colleagues who performed candid and valuable reviews of the original manuscripts. The publishing staffs of Springer are gratefully acknowledged for their enthusiasms and constant cooperation and help in bringing out this book.

The Editors

Dr. Diganta Bhusan Das, *Department of Engineering Science, The University of Oxford, Oxford OX1 3PJ, UK.*

Professor S.M. Hassanizadeh, *Department of Earth Sciences, Utrecht University, 3508 TA Utrecht, The Netherlands.*

Transp Porous Med (2005) 58:5–22
DOI 10.1007/s11242-004-5466-4

Bundle-of-Tubes Model for Calculating Dynamic Effects in the Capillary-Pressure-Saturation Relationship

HELGE K. DAHLE[1,*], MICHAEL A. CELIA[2] and S. MAJID HASSANIZADEH[3]
[1]*Department of Mathematics, University of Bergen, Johns Brungst. 12, N-5008 Bergen, Norway*
[2]*Department of Civil and Environmental Engineering, Princeton University*
[3]*Department of Earth Sciences, Utrecht University*

(Received: 18 August 2003; in final form: 27 April 2004)

Abstract. Traditional two-phase flow models use an algebraic relationship between capillary pressure and saturation. This relationship is based on measurements made under static conditions. However, this static relationship is then used to model dynamic conditions, and evidence suggests that the assumption of equilibrium between capillary pressure and saturation may not be be justified. Extended capillary pressure–saturation relationships have been proposed that include an additional term accounting for dynamic effects. In the present work we study some of the underlying pore-scale physical mechanisms that give rise to this so-called dynamic effect. The study is carried out with the aid of a simple bundle-of-tubes model wherein the pore space of a porous medium is represented by a set of parallel tubes. We perform virtual two-phase flow experiments in which a wetting fluid is displaced by a non-wetting fluid. The dynamics of fluid–fluid interfaces are taken into account. From these experiments, we extract information about the overall system dynamics, and determine coefficients that are relevant to the dynamic capillary pressure description. We find dynamic coefficients in the range of $10^2 - 10^3\,\mathrm{kg\,m^{-1}\,s^{-1}}$, which is in the lower range of experimental observations. We then analyze certain behavior of the system in terms of dimensionless groups, and we observe scale dependency in the dynamic coefficient. Based on these results, we then speculate about possible scale effects and the significance of the dynamic term.

Key words: two-phase flow in porous media, dynamic capillary pressure, pore-scale network models, bundle-of-tubes, volume averaging

1. Introduction

Traditional equations that describe two-phase flow in porous media are based on conservation equations which are coupled to material-dependent

*Author for correspondence: e-mail: reshd@mi.uib.no

constitutive equations. One of the traditional constitutive equations is an algebraic relationship between capillary pressure, P_c (the difference between equilibrium phase pressures) and fluid phase saturation, S_α (the fraction of void space occupied by the fluid phase α). While this constitutive relationship is typically highly complex, including nonlinearity and hysteresis as well as residual phase saturations, it is nonetheless algebraic. The algebraic nature means that a change in one of the variables implies an instantaneous change in the other, such that the relationship between P_c and S is an equilibrium relationship. For an equilibrium relationship to be appropriate, the time scale of any dynamics associated with the processes that govern the relationship must be fast relative to the dynamics associated with other system processes. Time scales to reach equilibrium in laboratory experiments (Stephens, 1995) make this assumption questionable.

Recently, the relationship between P_c and S has been generalized, based on thermodynamic arguments by Gray and Hassanizadeh (see Hassanizadeh and Gray, 1990, 1993a, b; Gray and Hassanizadeh, 1991a, b). The extended relationship reads:

$$(p^{nw} - p^w) - P_c(S_w) = f\left(S_w, \frac{\partial S_w}{\partial t}\right), \tag{1}$$

where f denotes an unspecified function depending on saturation and its rate of change. Their contention is that this condition includes dynamic effects and is valid under unsteady state and nonequilibrium conditions. This kind of relationship has previously been considered by Stauffer (1978), and similar results occur in the classic book by Barenblatt *et al.* (1990), see also Silin and Patzek (2004). Dynamic effects may also occur as a consequence of upscaling of effective parameters in two-phase flow, see Bourgeat and Panfilov (1998). Recently, Hassanizadeh *et al.* (2002) analyzed experimental data sets from the literature and showed that dynamic effects are present in standard laboratory experiments to determine P_c as a function of S, although most laboratory experiments are designed to avoid dynamic effects by using small pressure increments. Hassanizadeh *et al.* (2002) and Dahle *et al.* (2002) also showed that this new relationship can easily be included in numerical simulations, and that effects on problems involving infiltrating fluid fronts could be significant, if the dynamic coefficient exhibits scale dependence.

In the present work, we consider some of the underlying physical mechanisms that give rise to this so-called dynamic effect. To do this, we analyze a simple bundle-of-tubes model that represents the pore space of a porous medium. This model is analogous to the recent model of Bartley and Ruth (1999, 2001), who used a bundle-of-tubes model to analyze dynamic effects in relative permeability, Bartley and Ruth (2001) also presented initial calculations on dynamic effects on the $P_c - S$ relationship.

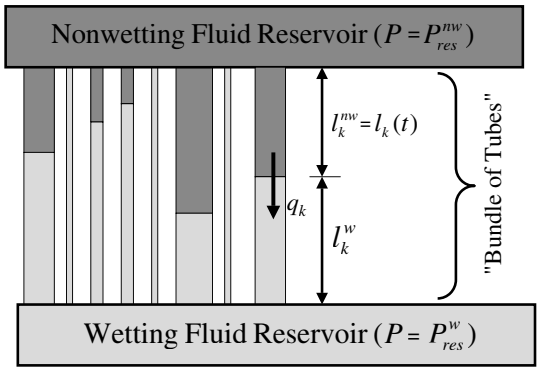

Figure 1. Bundle-of-tubes model.

In the model we present herein, we use a bundle-of-tubes model to analyze system behavior in the context of Figure 1. We perform virtual two-phase displacement experiments and mathematically track the dynamics of each fluid–fluid interface in two-fluid displacement experiments. From this we extract information about the overall system dynamics, and determine coefficients that are relevant to the dynamic description. We analyze certain behavior of the system in terms of dimensionless groups. Based on those results, we then speculate about possible scale effects and the significance of the dynamic term.

The paper is organized as follows. In the next section, we present background equations that are relevant to the derivations and calculations that follow. In the following section, we present the bundle-of-tubes model that is used to calculate system dynamics. We then describe the numerical experiments performed, and proceed to investigate certain scaling dependencies on the dynamic term. We end with a summary of the main findings and a discussion section.

2. Background Equations

The new relationship between P_c and S introduces a so-called dynamic capillary pressure, and hypothesizes that the rate of change of saturation is a function of the difference between the dynamic capillary pressure and the static, or equilibrium, capillary pressure. Assuming that a linear relationship holds, one will have, (Hassanizadeh and Gray, 1990):

$$-\tau \frac{\partial S_w}{\partial t} = P_c^{dyn} - P_c^{stat}(S_w). \tag{2}$$

In Equation (2), P_c^{stat} is the static or equilibrium capillary pressure, taken to be the capillary pressure that is traditionally measured in equilibrium pressure cell tests, see for example Stephens (1995); τ is a coefficient that

we will call the 'dynamic coefficient'; and P_c^{dyn} is the dynamic capillary pressure, defined as the difference between the volume-averaged pressure in the nonwetting phase and that in the wetting phase, viz.

$$P_c^{dyn} = \langle p^{nw} \rangle - \langle p^{w} \rangle, \tag{3}$$

where the angular brackets imply volume averaging. Notice that the averaging procedure introduces a length (and time) scale, so that the definition of (3) will be linked to these scales of averaging. The dynamic coefficient may still be a function of saturation as well as fluids and solid properties. Stauffer (1978) has suggested the following scaling of the dynamic coefficient:

$$\tau = \frac{\phi \mu}{k} \frac{\alpha}{\lambda} \left(\frac{p^e}{\rho g} \right)^2, \tag{4}$$

where k is the intrinsic permeability, μ and ρ are the viscosity and density of the (wetting) fluid, g is the gravity constant, $\alpha = 0.1$ and λ, p^e are coefficients in the Brook–Corey formula.

Ideally, in order to investigate the validity of Equations (2) and (4), one should perform a large number of experiments, in which fluid pressures and saturation should be measured under a number of different conditions and for a variety of soil and fluid combinations. That, however, would be extremely costly and time consuming. At these early stages of research on dynamic capillary effects, it would be useful to carry out some theoretical work in order to gain insight into the various aspects of this phenomenon. Thus, in this paper, we try to gain insight into the underlying physics of Equation (2) and the effect of various soil and fluid properties on the value of τ. We carry out this work by studying fluid–fluid displacement at the pore scale within a simple pore-scale network model, composed of a bundle of capillary tubes. A schematic of the system is shown in Figure 1.

Consider a single capillary tube, with one end of the tube connected to a non-wetting-phase reservoir and the other end connected to a wetting-phase reservoir. The corresponding reservoir pressures are denoted by P_{res}^{nw} and P_{res}^{w}, respectively. Assume that both reservoir pressures may be controlled, and are set so that their difference is given by $\Delta P = P_{res}^{nw} - P_{res}^{w}$. If the tube has radius r, and is initially filled with wetting fluid, then non-wetting fluid will invade the tube if the pressure difference exceeds the displacement pressure given by the Young-Laplace criterion (Dullien, 1992) $\Delta P > 2\sigma^{wn} \cos\theta / r$, where σ^{wn} denotes interfacial tension between the wetting and non-wetting fluids, and θ is contact angle. Once this occurs, the fluid movement may be approximated by the Washburn equation (Washburn, 1921):

$$q = dl/dt = -\frac{r^2}{8\bar{\mu}(l)L}(-\Delta P + \bar{\rho}(l) L g \sin\Phi + p_c(r)). \tag{5}$$

In Equation (5), $\bar{\mu}$ and $\bar{\rho}$ are length-averaged viscosity and density, respectively, of the fluids within the tube, $l = l(t)$ is the position of the interface in the tube of length L, Φ is the angle the tube makes with the vertical, and p_c is the local capillary pressure, taken to be equal to the displacement pressure,

$$p_c(r) = \frac{2\sigma^{wn} cos\theta}{r}, \tag{6}$$

To motivate the use of a bundle-of-tubes model, and to show the connection to the larger (continuum–porous-medium) scale, consider the following simple scaling argument. Assume Equations (5) and (6), applied to a large collection of pore tubes of different radii, govern the fluid flow through some portion of a porous medium. Then the analogies between the small-scale quantities in Equations (5) and (6), and those defined at the continuum-porous-medium scale, may be identified, under both static and dynamic conditions, as:

$$\begin{array}{lll} PS: & \dfrac{dl}{dt} & = -\dfrac{r^2}{8\bar{\mu}(l)L} \qquad (\underbrace{-\Delta P + \bar{\rho}(l) L g \sin\Phi}_{\downarrow} + \underset{\downarrow}{p_c}) \\ & \downarrow & \\ CS: & -\dfrac{dS_w}{dt} & = -\dfrac{1}{\tau} \qquad\quad (\qquad -P_c^{dyn} \qquad + P_c^{stat}) \end{array}$$

Here PS denotes 'pore scale' and CS denotes 'continuum scale'. We see the direct correspondence between the dynamic displacement and the interface movement, and the associated upscaled versions of average phase pressure evolution and phase saturation changes. In particular, both $dl/dt = 0$ and $dS_w/dt = 0$ at equilibrium, although the units are different due to volume averaging. This provides motivation to use a bundle-of-tubes model to investigate more complex aspects of dynamic phase pressures, the associated dynamic capillary pressure, and its relationship to saturation dynamics. For more details on the use of these ideas in conjunction with pore-scale network models, we refer to Dahle and Celia (1999) and Hassanizadeh *et al.* (2002).

3. Bundle-of-Tubes Model

3.1. VOLUME AVERAGING

One of the main advantages of pore-scale network models is that variables that are difficult or impossible to measure physically can be computed directly from the network model. In the present case, we are interested in calculation of volume-averaged phase pressures, local and averaged capillary pressure, averaged phase saturations, and local interfacial velocities

and associated changes in average phase saturations. To perform these calculations, we let V denote an averaging volume within the domain of the pore-scale network model, and introduce the indicator function γ defined by

$$\gamma_\alpha(\mathbf{x}, t) = \begin{cases} 1 \text{ if phase } \alpha \text{ at } (\mathbf{x}, t), \\ 0 \text{ otherwise.} \end{cases} \tag{7}$$

We then define

$$V_p = \iiint_V (\gamma_{nw} + \gamma_w) d\mathbf{x}, \;\; V_w(t) = \iiint_V \gamma_w(\mathbf{x}, t) d\mathbf{x}, \tag{8}$$

and

$$V_{nw}(t) = V_p - V_w(t). \tag{9}$$

Here V_p is the total pore space of the averaging volume, $\phi = V_p / V$ is the porosity, and $V_\alpha(t)$ is the pore space occupied by phase α, with $\alpha = w$ for the wetting phase and $\alpha = nw$ for the non-wetting phase. Average state variables like saturation and phase pressures can now be defined as follows:

$$S_w(t) = \frac{V_w(t)}{V_p} = 1 - S_{nw}(t), \tag{10}$$

$$\langle p^\alpha \rangle = \frac{\iiint_V p_\alpha(\mathbf{x}, t) \gamma_\alpha(\mathbf{x}, t) d\mathbf{x}}{\iiint_V \gamma_\alpha(\mathbf{x}, t) d\mathbf{x}}, \;\; \alpha = w, nw. \tag{11}$$

The bracket notation $\langle\rangle$ is used to denote average.

3.2. GEOMETRY OF THE BUNDLE-OF-TUBES MODEL

The bundle-of-tubes pore-scale model represents the pore space by a number, N, of non-intersecting capillary tubes. Each tube has length L, with one end of the tube connected to a reservoir of nonwetting fluid and the other end connected to a reservoir of wetting fluid (see Figure 1). Each tube is assigned a different radius r, with the radii drawn from a cut-off log-normal distribution

$$f(r; \sigma_{nd}) = \frac{\sqrt{2} \exp\left[-\frac{1}{2} \left(\frac{\ln \frac{r}{r_{ch}}}{\sigma_{nd}} \right)^2 \right]}{\sqrt{\pi \sigma_{nd}^2}\, r \left[\operatorname{erf}\left(\frac{\ln \frac{r_{\max}}{r_{ch}}}{\sqrt{2\sigma_{nd}^2}} \right) - \operatorname{erf}\left(\frac{\ln \frac{r_{\min}}{r_{ch}}}{\sqrt{2\sigma_{nd}^2}} \right) \right]}. \tag{12}$$

Here r_{ch} and σ_{nd} are the mean and variance of the parent distribution. We have conveniently fixed the maximum and minimum radius to be

$r_{\max} = 10^2 r_{ch}$ and $r_{\min} = 10^{-3} r_{ch}$. Following Dullien (1992), let $V = L^3$ be the averaging volume of the bundle, and define the average of the pth power of r_k by:

$$\langle r^p \rangle = \sum_{k=1}^{N} r_k^p / N. \tag{13}$$

Then the porosity is given by

$$\phi = \frac{V_p}{L^3} = \frac{\pi N \langle r^2 \rangle}{L^2}, \text{ or } L = \left(\frac{\pi N \langle r^2 \rangle}{\phi} \right)^{1/2}, \tag{14}$$

In our computations we will specify the porosity ϕ and calculate the length of the tubes L from this formula. From the parallel tubes model, we may calculate an intrinsic permeability, k, for the bundle as

$$\left.\begin{aligned} Q &= \textstyle\sum_k \frac{\pi r_k^4}{8\mu} \frac{\Delta P}{L} = \frac{\pi N \langle r^4 \rangle}{8\mu} \frac{\Delta P}{L} \\ Q &= \frac{k L^2}{\mu} \frac{\Delta P}{L} \end{aligned}\right\} \Rightarrow k = \frac{\phi \langle r^4 \rangle}{8 \langle r^2 \rangle}, \tag{15}$$

where we have used Equation (14).

3.3. COMPUTATIONAL ALGORITHM

Assume that the tubes are ordered by decreasing radius such that $r_k \geqslant r_{k+1}$, $k = 1, 2, \ldots, N-1$, and that they are initially filled by wetting fluid. The bundle is then drained by gradually increasing the non-wetting reservoir pressure P_{res}^{nw}, while the wetting reservoir pressure, P_{res}^{w}, is kept fixed, say equal to zero. The dynamics of each interface is assumed to be governed by Equation (5). However, in order to save on algebra, the gravity will be neglected in the following analysis and the two fluids are assumed to have the same viscosity μ, leading to a pressure distribution within the tube as shown in Figure 2. Thus, once the non-wetting reservoir pressure exceeds the displacement pressure of tube k, the location of that interface at any time t, $l = l_k(t)$, is given by,

$$l_k(t) = q_k \cdot (t - t_0) + l_k^0, \tag{16}$$

where

$$q_k = -\frac{r_k^2}{8\mu L}(-\Delta P + p_c(r_k)), \tag{17}$$

and l_k^0 is the position of the interface at time t_0. When the interface reaches the wetting reservoir, $l_k = L$, that interface will be considered to be trapped, with $q_k = 0$, and the pressure in the corresponding drained tubes is kept

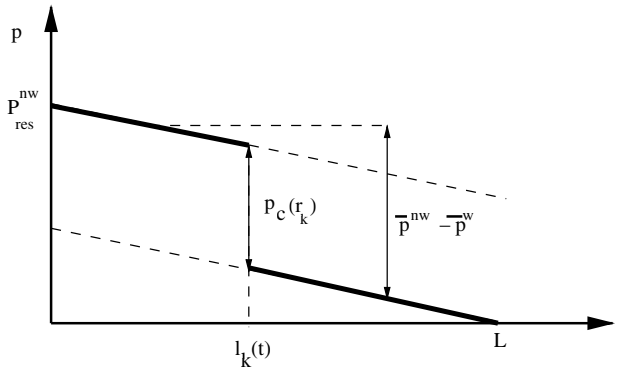

Figure 2. Pressure distribution in a single tube containing two fluids of equal viscosity separated by an interface located at $l = l_k(t)$.

constant at P_{res}^{nw}. By averaging we obtain the following expression for the saturation of the wetting phase at any given time t:

$$S_w(t) = \frac{V_w(t)}{V_p} = 1 - \frac{\sum_k \pi r_k^2 l_k}{V_p}. \tag{18}$$

The time derivative of this saturation is

$$\frac{dS_w}{dt} = -\frac{1}{V_p}\sum_k \pi r_k^2 \frac{dl_k}{dt} = -\frac{1}{V_p}\sum_k \pi r_k^2 q_k. \tag{19}$$

By using Equation (11) we obtain the average phase pressures ($\alpha = w, nw$):

$$< p^\alpha >= \frac{1}{V_\alpha(t)}\sum_k \pi r_k^2 l_k^\alpha (\pm\frac{1}{2}\Delta p_k^\alpha + P_{res}^\alpha), \tag{20}$$

where

$$\Delta p_k^\alpha = \begin{cases} \frac{l_k^\alpha}{L}(-\Delta P + p_c(r_k)), & 0 < l_k^\alpha < L; \\ 0 & l_k^\alpha = L. \end{cases} \tag{21}$$

Here $l_k^{nw} = l_k(t)$, $l_k^w = L - l_k(t)$ and the plus sign is chosen if $\alpha = nw$. These phase pressures are then used in Equation (3) to define the dynamic capillary pressure. At equilibrium the capillary pressure over an interface has to exactly balance the boundary pressures. This leads to the following definition of a static capillary pressure:

$$P_c^{\text{stat}}(S_w) = p_c(r_k),\ S_w^{k-1} \le S_w \le S_w^k \text{ with } S_w^k = 1 - \frac{\sum_i^{k-1} \pi r_i^2 L}{V_p}. \tag{22}$$

Note that P_c^{stat} is defined stepwise as the displacement pressure of successive tubes. In Figure 3 dynamic and static capillary-pressure–saturation

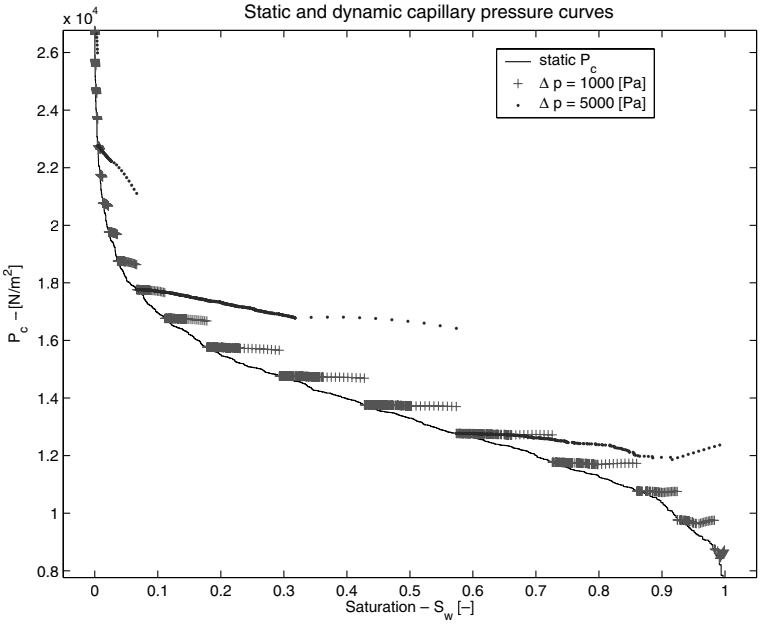

Figure 3. Dynamic and static capillary-pressures–saturation curves.

relationships are compared for two different drainage experiments. The only difference between these experiments is that different pressure increments, Δp_{step}, are used to update the nonwetting reservoir pressure P_{res}^{nw}.

Observe that the dynamic capillary-pressure curves in Figure 3 are always above the static curve, which is consistent with the theory leading to Equation (2). Another interesting feature of this Figure is the non monotonicity of the dynamic P_c-curve for large saturation. Similar behavior has also been observed in dynamic network simulations, e.g. Hassanizadeh *et al.* (2002). To explain the behavior in Figure 3, consider a single tube, k, with a moving interface at $l = l_k(t)$. Since the viscosities of the fluids are equal, the pressure gradient has to be equal within each fluid phase of the tube, see Figure 2, and the average phase pressures in that tube are given by:

$$\bar{p}_k^{nw} = P_{\text{res}}^{nw} - \frac{l_k}{2L}(P_{\text{res}}^{nw} - p_c(r_k)), \;\; \bar{p}_k^{w} = \frac{L - l_k}{2L}(P_{\text{res}}^{nw} - p_c(r_k)). \tag{23}$$

Thus, the average phase pressures in a single tube will decrease at the same rate, whereas the difference is constant in time:

$$\bar{p}_k^{nw} - \bar{p}_k^{w} = \frac{1}{2}(P_{\text{res}}^{nw} + p_c(r_k)). \tag{24}$$

If we consider the ensemble of tubes, the average phase pressures, Equation (20), may alternatively be written:

$$\langle p^{\alpha} \rangle = \frac{1}{V_{\alpha}(t)} \sum_{k} \bar{p}_{k}^{\alpha} V_{\alpha}^{k}, \tag{25}$$

where V_{α}^{k} is the volume occupied by phase α in tube k, $\bar{p}_{k}^{nw} = P_{res}^{nw}$ if the interface in tube k is trapped at $l_k = L$, and $\bar{p}_{k}^{w} = 0$ if the interface is trapped at $l_k = 0$. At high saturations we may assume that all the non-wetting fluid is associated with moving interfaces. Since the flow rate in each tube is constant, all the volumes associated with the non-wetting fluids are then changing proportional to time t. It follows that $\langle p^{nw} \rangle$ has to be decreasing function of time (i.e. decreasing saturation), since all the weights, $\bar{p}_{k}^{nw}$, are decreasing. At the point in time when interfaces starts to get trapped at the outflow boundary, the associated weights will increase, and $\langle p^{nw} \rangle$ may start to increase in time. On the other hand, for high saturations, the volumes occupied by the wetting fluid is mainly associated with interfaces that are immobile at the inflow boundary giving weights $\bar{p}_{k}^{w} = 0$, so that $\langle p^{w} \rangle \approx 0$. Thus, $P_{c}^{dyn} \approx \langle p^{nw} \rangle$ has to be a decreasing function with time in this case. By looking at Figure 3, this behavior is clearly apparent for $0.9 < S_w < 1$ and $\Delta p_{step} = 5000 Pa$. For $S_w \approx 0.9$ a sufficient number of interfaces become trapped at the outflow boundary, leading to a change of slope in the dynamic $P_c - S$ curve.

4. Numerical Experiments

In the numerical tests reported herein, a set of radii are generated based on the log-normal distribution, and these radii define one realization of the pore-scale geometry. For a given realization, the tubes are drained by imposition of step-wise changes in pressure in the nonwetting reservoir. Initially we choose $P_{\text{res}}^{nw} = p_c(r_1) + \Delta p_{\text{step}}$ and then increase P_{res}^{nw} subsequently by Δp_{step} each time an equilibrium is reached (meaning that no further interfaces will move). In this way the entire bundle is drained, and we can compute $P_{c}^{\text{stat}} - P_{c}^{\text{dyn}}$ and dS_w/dt at a given set of target saturations $S_{\text{target}} \in \{0.1, 0.2, \ldots, 0.9\}$. To obtain a sufficiently large number of data points at each target saturation we vary the pressure step according to

$$\Delta p_{\text{step}} = n \cdot \delta p, \;\; n = 1, 2, \ldots, N_{\text{step}}, \;\; \text{with } \delta p = (1.1 p_c(r_N) - p_c(r_1))/N_{\text{step}}.$$

Observe that the largest pressure increment is chosen such that the bundle will drain in a single step. We have chosen $N_{\text{step}} = 50$, and if nothing else is specified other parameters for the bundle are chosen as listed in Table I.

In Figure 4, $P_{c}^{\text{stat}} - P_{c}^{\text{dyn}}$ is plotted against dS_w/dt at target saturations 0.2, 0.5 and 0.8. Observe that the data points appear to behave linearly somewhat away from the origin, while close to the origin we have that $P_{c}^{\text{dyn}} \to P_{c}^{\text{stat}}$ as $dS_w/dt \to 0$ in a nonlinear fashion. We may fit a straight line through the linear portion of the curve, with parameters τ and β defined as slope and intercept,

Table I. Parameters for bundle of tube model. Length L of tubes and intrinsic permeability k are calculated from one realization of the bundle using Equations (14) and (15)

Parameter	Description	Value
N	Number of tubes	1000
N_{step}	Number of pressure increments	50
r_{ch}	Mean value pore-size distribution	10^{-5} [m]
$r_{\min}$	Lower cut-off radius	$10^{-3} r_{ch}$
$r_{\max}$	Upper cut-off radius	$10^{2} r_{ch}$
σ_{nd}	Variance of pore-size distribution	0.2
μ	Viscosity	0.5×10^{-2} [kg m^{-1} s^{-1}]
σ^{wn}	Surface tension	7.2×10^{-2} [kg s^{-2}]
θ	Contact angle	0 (radians)
ϕ	Porosity	0.3
L	Length	$\sim 10^{-3}$ [m]
k	Permeability	$\sim 4.8 \times 10^{-12}$ [m^2]
τ	Dynamic coefficient	~ 274 [kg m^{-1} s^{-1}]
β	Intercept	$\sim 1.5 \times 10^{3}$ [kg m^{-1} s^{-2}]

Similarly, the dynamic coefficient τ and the intercept β is calculated from the same realization at saturation $S_w = 0.5$

$$-\tau \partial S_w / \partial t + \beta = P_c^{\text{dyn}} - P_c^{\text{stat}}, \tag{26}$$

where $\tau > 0$, $\beta > 0$ may be functions of S_w and other parameters. Based on Stauffer's formula (4) we may conjecture that

$$\tau k / \phi \mu L^2 = \Pi_\tau(S_w, \sigma_{nd}). \tag{27}$$

Here L should be interpreted as a characteristic length scale associated with the averaging volume. We also conjecture that

$$\beta / \sigma_{nd} P_c^{ch} = \Pi_\beta(S_w), \tag{28}$$

where $P_c^{ch} = 2\sigma^{wn} cos\theta / r_{ch}$ and r_{ch} is the mean of the pore size distribution.

To determine values of the parameters τ and β, and to test the conjectures put forth in Equations (27) and (28), we run a series of numerical experiments and analyze the results. As part of this analysis, we determine a regression line through the linear part of the plots (see for example Figure 4). To compute the regression line in a systematic manner, the data points are first normalized to fall within the interval $[-1, 0]$. A regression line is then calculated for all data points associated with $dS_w/dt < -0.3$ on the normalized plot. The regression line is then transformed back to the original coordinate system. The slope of the line gives the estimate for τ while the intercept gives β. Note that $\beta \neq 0$ corresponds to existence of a

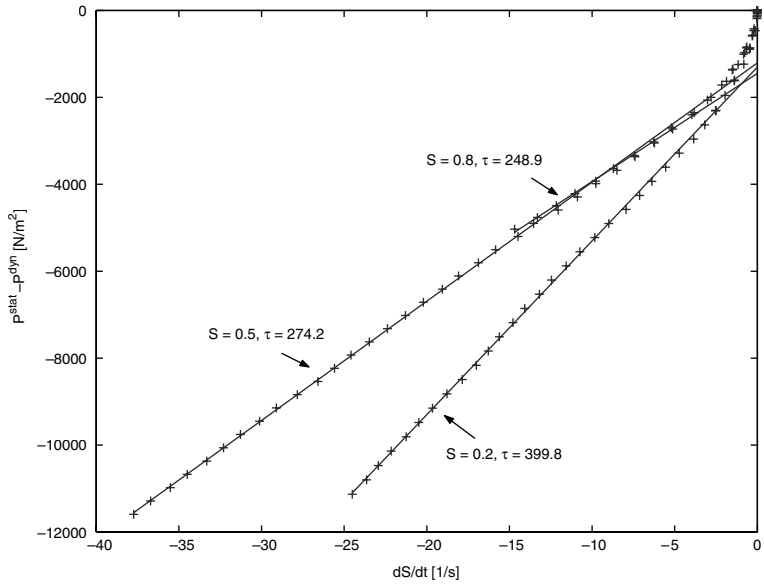

Figure 4. $P_c^{stat} - P_c^{dyn}$ versus dS_w/dt at saturations $S_w = 0.2, 0.5, 0.8$.

nonlinear region near the origin. The magnitude of β reflects the degree of this nonlinearity. In all our simulations, the slope of the regression line has been positive and the *curvature* of the data points have been such that the vertical axis intersection has been below the origin.

The proposed conjectures can now be tested by systematically varying the parameters associated with our bundle-of-tubes model. For each new value of a specified parameter, a new realization of the bundle is generated and this bundle is then drained using the N_{step} different pressure steps to obtain regression lines as in Figure 4. The parameters that are varied are N (number of tubes), ϕ (porosity), μ (viscosity), r_{ch} (mean pore-size distribution), σ_{nd} (variance of pore-size distribution), and θ (contact angle). Note that varying θ is equivalent to varying the surface tension σ^{wn}. It is also

Table II. Results from varying different parameters, keeping the others fixed as in Table I

Parameter	Range	k	L	τ	β
N	200–10,000	4.77×10^{-12}	$N^{1/2}$	N	*indep.*
ϕ	0.05–0.45	ϕ	$\phi^{-1/2}$	$\phi^{-1/2}$	*indep.*
r_{ch}	$10^{-6} - 10^{-4}$	r_{ch}^2	r_{ch}	*indep.*	r_{ch}^{-1}
μ	$10^{-4} - 10^{-1}$	4.79×10^{-12}	0.11×10^{-2}	μ	*indep.*
θ	$0 - 1.5608$	4.79×10^{-12}	0.11×10^{-2}	*indep.*	$\cos\theta$
σ_{nd}	$0.1 - 0.6$	*	*	*	σ_{nd}

The symbol * means that no obvious power law was found.

possible to vary the lower- and upper-cut-off radius $r_{\min}$ and $r_{\max}$ independently. However, for this study they are kept constant with values as given in Table I. The findings of our numerical simulations are summarized in Table II. For example, the number of tubes is increased from $N = 200$ to $N = 10000$ with step size 200 tubes. As expected, we observe that the permeability $k \sim 4.77 \times 10^{-12}[\mathrm{m}^2]$ is essentially constant, i.e: k varies randomly around a mean value of $4.77 \times 10^{-12}[\mathrm{m}^2]$ for various realizations of the bundle. Furthermore, $L \sim N^{1/2}$, and $\tau \sim N$, whereas β is essentially independent of N as $N = 200, 400, \ldots, 10,000$. Similar results are tabulated when varying the other parameters, see Table II. However, it turns out that the variance of the pore-size distribution σ_{nd}, is a special parameter. We let σ_{nd} vary linearly between $\sigma_{nd} = 0.1$ and $\sigma_{nd} = 0.6$ using 50 steps. Both k and L increase with σ_{nd} but no obvious power law dependency is found. Similarly, we find no obvious dependency with respect to τ and σ_{nd}. In fact, τ-values for smaller saturations increase with respect to σ_{nd} whereas they decrease at the larger saturation values. On the other hand it appears that $\beta \sim \sigma_{nd}$, although the fluctuations in the data points are fairly large for the larger values of σ_{nd}.

For each parameter that is varied, we have plotted the mean value for the dimensional groupings Π_τ and Π_β at the specified target saturations, see Figures 5–7. The error bars in these plots give the variance of the fluctuations around the mean value, due to different realizations of the

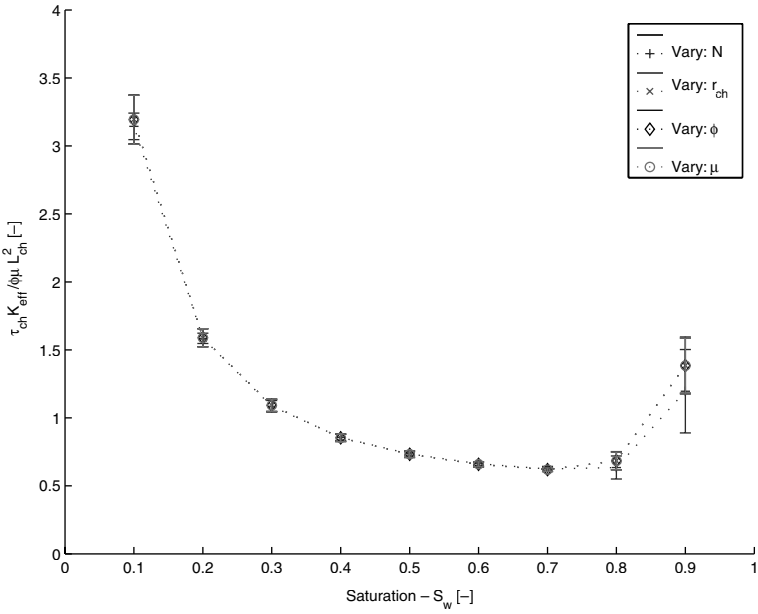

Figure 5. Dimensional grouping $\Pi_\tau(S_w, \sigma_{nd}) = \tau k/\phi\mu L^2$ as a function of saturation is fixed at $\sigma_{nd} = 0.2$. Variance of the pore-size distribution is fixed at $\sigma_{nd} = 0.2$.

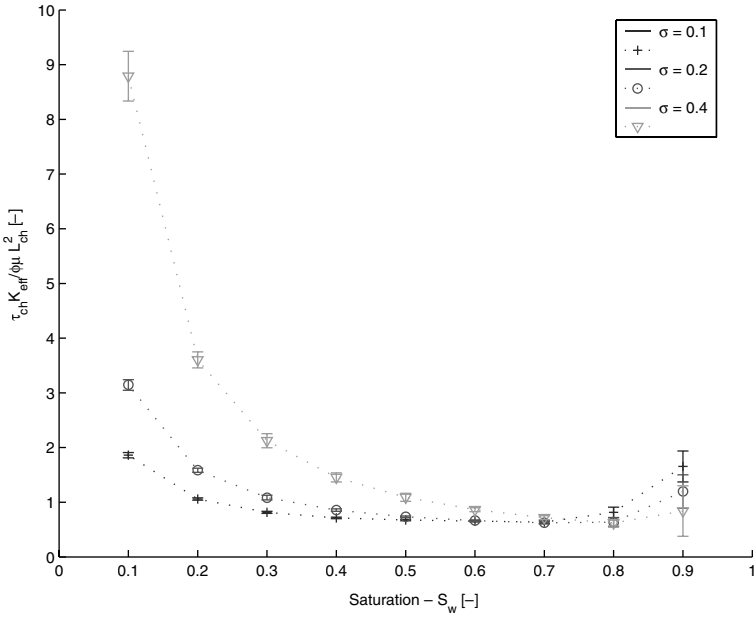

Figure 6. Dimensional grouping $\Pi_\tau(S_w, \sigma_{nd}) = \tau k/\phi\mu L^2$ as a function of saturation. Each curve represents a different variance of the pore-size distribution: $\sigma_{nd} =$ 0.1, 0.2, 0.4.

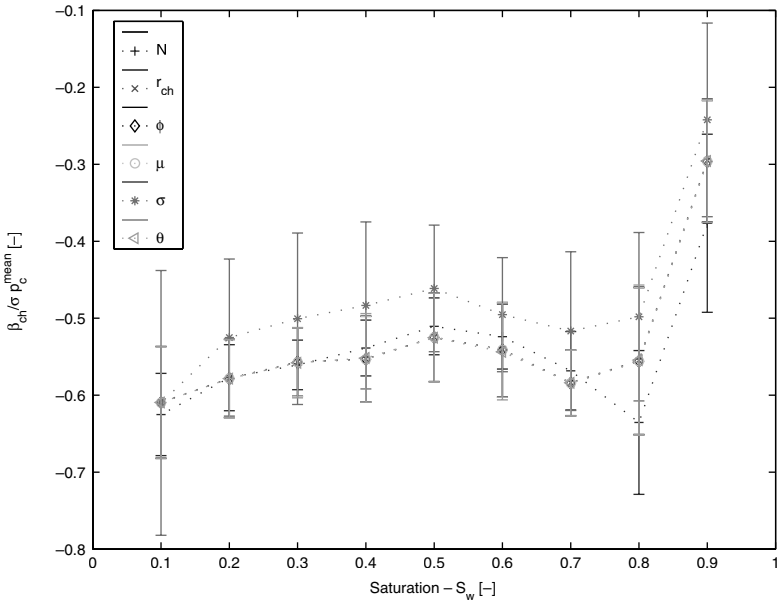

Figure 7. Dimensional grouping $\Pi_\beta(S_w) = \beta/\sigma_{nd} P_c^{ch}$ as a function of saturation.

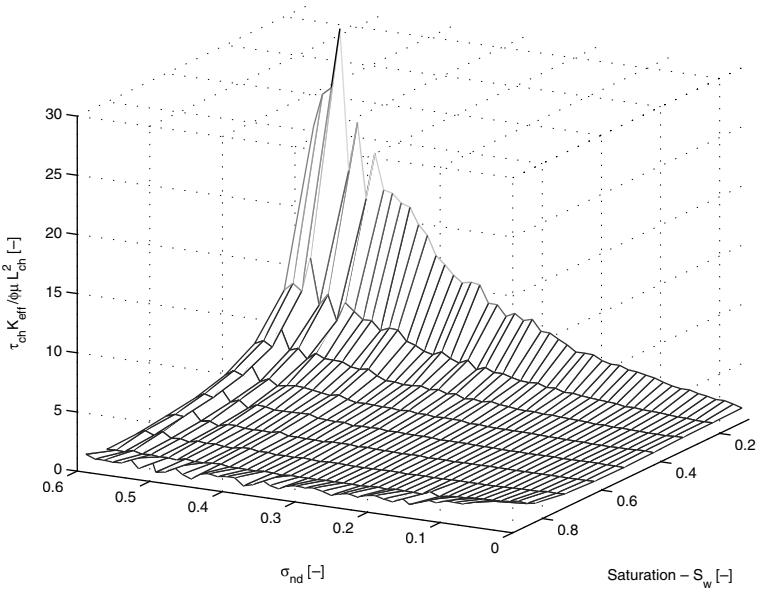

Figure 8. Dimensional grouping $\Pi_\tau(S_w, \sigma_{nd}) = \tau k/\phi\mu L^2$ as a function of saturation and variance of the pore-size distribution.

bundle for each update of the a specific parameter. We observe that Figures 5 and 7 reconcile the parameter dependencies of Π_τ and Π_β fairly well. In Figure 8, we do not include the data related to varying the variance of the pore-size distribution, simply because we are not able to make this parameter fit into the dimensional grouping of Π_τ. In Figure 6, we have plotted the dimensional grouping Π_τ when the number of tubes N is varied from $N = 200$ to $N = 10,000$, and for three different values of σ_{nd}. This Figure illustrates the difficulty associated with the parameter σ_{nd}. We are simply not able to include σ_{nd} into the dimensional grouping Π_τ to make this independent of σ_{nd}, because the dependency of this parameter is coupled to the saturations. We therefore suggest that $\Pi_\tau = \Pi_\tau(S_w, \sigma_{nd})$. This surface is plotted in Figure 8. A possible explanation for the more complicated dependency on σ_{nd} is related to the observation that $\tau \sim k^{-1}$. When σ_{nd} is increased we get more tubes with smaller and larger radius. This means that when we estimate τ for larger saturations the 'local' permeability over that section of the bundle must increase with σ_{nd}. Since τ is inversely proportional to permeability we should therefor expect τ to decrease for larger saturations when σ_{nd} is increased. On the other hand for smaller saturations the 'local' permeability should decrease with σ_{nd} resulting in an increase in τ.

Finally, by Equation (27), we have that

$$\tau(S_w) = \frac{\phi \mu L^2}{k} = \Pi_\tau(S_w), \tag{29}$$

for a fixed variance of the pore-size distribution σ_{nd}. Hence, from Figure 5, it follows that the dynamic coefficient τ is a decreasing function of saturation except for larger values of S_w, where τ is an increasing function.

5. Summary and Discussion

In this paper we have investigated *dynamic* effects in the capillary pressure–saturation relationship using a bundle-of-tubes model. At the pore-scale, fluid–fluid interfaces will always move to produce an equilibrium between external forces and internal forces created by surface tension over the interfaces. Because of viscosity, interfaces require a finite relaxation time to achieve such an equilibrium. This dynamics of interfaces at the pore-scale may for example be described by the Washburn Equation (5). This is a simple model and the corresponding dynamic effect is expected to be small. The calculated value of τ ($\sim 274\,\mathrm{kg\,m^{-1}\,s^{-1}}$) is indeed very small. For a more complicated pore-scale network model, larger values for τ are obtained. For example, for a three-dimensional pore-scale network model Gielen *et al.* (2004) obtained values of order $10^4 - 10^5\,\mathrm{kg\,m^{-1}\,s^{-1}}$. When micro-scale soil heterogeneities are taken into account, even larger values for τ are found. For example, experimental results reported by Manthey *et al.* (2004) on a 6-cm long homogeneous soil sample yield a τ-value of about $10^5\,\mathrm{kg\,m^{-1}\,s^{-1}}$. At even larger scales, dynamics of interfaces must be associated with the time scale of changes in phase saturations.

Our analysis of the bundle-of-tubes model leads to the relationship (26) involving a dynamic coefficient τ and an intercept of the vertical axis β. We have investigated dimensionless groupings (27) and (28) containing τ and β, respectively. The dimensionless grouping involving τ shows a clear dependency on saturation, in particular for larger values of the variance of the pore-size distribution. It also shows that the dynamic coefficient τ increases as the square of the length scale L associated with the averaging volume. This suggest that the dynamic coefficient may become arbitrarily large as the averaging volume increases in size. However, we suspect that the length scale has to be tied to typical length scales associated with the problem under consideration, e.g. length scales associated with moving fronts, and not necessarily the length scale of the averaging volumes. We will investigate the dependency of τ with respect to typical length scales in future work. The dynamic effect observed in our bundle-of-tubes model is only due to the motion of single interfaces. The effect would have been larger if effects such as hysteresis in contact angle would have been

included; e.g. a smaller contact angle during drainage compared to when the interface is at rest.

The relationship (26) may not be valid for small temporal changes in saturation due to the nonlinearity introduced by local capillary pressure. The magnitude of this nonlinearity is reflected in the size of the vertical axis intercept β. In fact, the dimensionless grouping involving β shows that this intercept is proportional to surface tension and contact angle of the fluid–fluid interface. On the other hand, the dimensionless grouping that contains β does not show any clear dependency on the saturation. If this turns out to be the case, the β-term may have no importance with respect to continuum scale models.

Acknowledgements

Partial support for this work was provided to H.K. Dahle by the Norwegian Research Council and Norsk Hydro under Grants 151400/210 and 450196, to M.A. Celia by the National Science Foundation under Grant EAR-0309607, and the research by S.M. Hassanizadeh has been carried out in the framework of project no. NOW/ALW 809.62.012 financed by the Dutch Organization for Scientific Research.

References

Barenblatt, G. I., Entov, V. M. and Ryzhik, V. M.: 1990, *Theory of Fluids Through Natural Rocks*, Kluwer Academic Publishing: Dordrecht.

Bartley, J. T. and Ruth, D. W.: 1999, Relative permeability analysis of tube bundle models, *Transport Porous Media* **36**, 161–187.

Bartley, J. T. and Ruth, D. W.: 2001, Relative permeability analysis of tube bundle models, including capillary pressure, *Transport Porous Media* **45**, 447–480.

Bourgeat, A. and Panfilov, M.: 1998, Effective two-phase flow through highly heterogeneous porous media: capillary nonequilibrium effects, *Comput. Geosci.* **2**, 191–215.

Dahle, H. K. and Celia, M.: 1999, A dynamic network model for two-phase immiscible flow, *Comput. Geosci.* **3**, 1–22.

Dahle, H. K., Celia, M. A., Hassanizadeh, S. M. and Karlsen, K. H.: 2002, A total pressure–saturation formulation of two-phase flow incorporating dynamic effects in the capillary-pressure–saturation relationship. In: *Proc. 14th Int. Conf. on Comp. Meth. in Water Resources, Delft, The Netherlands, June 2002*.

Dullien, A.: 1992, *Porous Media: Fluid Transport and Pore Structure*, Academic Press, 2nd edn. New York.

Gielen, T., Hassanizadeh, S. M., Leijnse, A., and Nordhaug, H. F.: 2004, *Dynamic Effects in Multiphase Flow: A Pore-Scale Network Approach*. Kluwer Academic Publisher.

Gray, W. and Hassanizadeh, S.: 1991a, Paradoxes and Realities in Unsaturated Flow Theory, *Water Resour. Res.* **27**(8), 1847–1854.

Gray, W. and Hassanizadeh, S.: 1991b, Unsaturated flow theory including interfacial phenomena. *Water Resour. Res.* **27**(8), 1855–1863.

Hassanizadeh, S., Celia, M. and Dahle, H.: 2002, Dynamic effects in the capillary pressure–saturation relationship and its impacts on unsaturated flow, *Vadose Zone J.* **1**, 38–57.